Geomechanics and Engineering, *Vol. 35, No. 4 (2023) 425-436*
https://doi.org/10.12989/gae.2023.35.4.425

Polynomial model controlling the physical properties of a gypsum-sand mixture (GSM)

Seunghwan Seo[a] and Moonkyung Chung*

Department of Geotechnical Engineering Research, Korea Institute of Civil Engineering and Building Technology (KICT), Goyang, Gyeonggi 10223, Republic of Korea

(*Received April 6, 2022, Revised October 14, 2023, Accepted November 6, 2023*)

Abstract. An effective tool for researching actual problems in geotechnical and mining engineering is to conduct physical modeling tests using similar materials. A reliable geometric scaled model test requires selecting similar materials and conducting tests to determine physical properties such as the mixing ratio of the mixed materials. In this paper, a method is proposed to determine similar materials that can reproduce target properties using a polynomial model based on experimental results on modeling materials using a gypsum-sand mixture (GSM) to simulate rocks. To that end, a database is prepared using the unconfined compressive strength, elastic modulus, and density of 459 GSM samples as output parameters and the weight ratio of the mixing materials as input parameters. Further, a model that can predict the physical properties of the GSM using this database and a polynomial approach is proposed. The performance of the developed method is evaluated by comparing the predicted and observed values; the results demonstrate that the proposed polynomial model can predict the physical properties of the GSM with high accuracy. Sensitivity analysis results indicated that the gypsum–water ratio significantly affects the prediction of the physical properties of the GSM. The proposed polynomial model is used as a powerful tool to simplify the process of determining similar materials for rocks and conduct highly reliable experiments in a physical modeling test.

Keywords: geometric scaled model; gypsum-sand mixture; physical modeling tests; polynomial approach; similar material

1. Introduction

Although the development of computational techniques facilitated wide-ranging analysis research in the geotechnical and mining engineering fields, physical modeling continues to play an indispensable role (Liu *et al*. 2003, Sterpi *et al*. 2004, Manzella *et al*. 2008). It is difficult to conduct large-scale complex projects in fields such as mine tunnels, and such projects can be investigated through theoretical analysis and numerical modeling. However, most of these modeling projects are performed using ground dynamic simulations using similar materials (Kim *et al*. 1998, Chapman *et al*. 2006, Lemaitre *et al*. 1985, He *et al*. 2010). This is a more economical and intuitive method to perform scaled physical model tests using similar materials because full-scale tests are costly and difficult to perform repeatedly (Harris and Sabnis 1999). However, selecting appropriate modeling materials to simulate rocks can be a challenging problem in the scaled physical model tests because the geometric simulation test expresses and tests real physical objects according to a certain proportional relationship with the prototype (similarity law). The modeling materials must have all or most of the major properties of the prototype and allow experimentation for a shorter time with a lower cost. Therefore, the selected modeling materials must have physical and mechanical properties similar to those of the prototype to obtain more reliable results (Huang *et al*. 2013).

To this end, various studies have been conducted for the development of materials such as concrete, plaster, gypsum, cork, rubber, plastics, and gelatins (Stimpson 1970, He *et al*. 2010, Dong *et al*. 2012, Huang *et al*. 2013, Zhang *et al*. 2008, Ma *et al*. 2004). For example, a synthetic soft rock was developed by Johnston and Choi (1986). A soft sedimentary rock composed of gypsum cement, fine sand, and water was also reported (Indraratna 1990). Subsequently, materials similar to rocks were developed for physical modeling by combining a material composed of quartz sand and barite and materials such as cement, gypsum, or lime. Ratios of sand, fly ash, and plaster gypsum comprising similar materials and their influencing factors were investigated (Chen *et al*. 2015). Scaled model tests of rocks often use mixed materials of gypsum and sand because gypsum is a homogeneous and isotropic soft synthetic rock; each batch in the laboratory conditions can easily reproduce the unchanging properties (Conley and Bundy 1958, Karni 1970). The raw materials (hydrated lime and fine sand) used for producing gypsum have the advantages of being easily available and economical, their properties change little after curing, and they are insensitive to room temperature and humidity changes. Furthermore, gypsum mixed with sand at an appropriate ratio provides highly reliable and convincing evidence for the adequacy of

*Corresponding author, Ph.D.
E-mail: mkchung@kict.re.kr
[a]Senior Researcher
E-mail: seunghwanseo@kict.re.kr

ISSN: 2005-307X (Print), 2092-6219 (Online)

various ground and rock dynamic modeling, which includes the model joints of sedimentary rock, soft rock, hard rock, and bedrock (Seo *et al*. 2021, Chung *et al*. 2013, Coquard and Boisetelle 1994, Hobbs 1968, Jung and Kim 2006, Lee and Jeong 2016, Indraratna *et al*. 1998 Yang and Chiang 2000, Jiang *et al*. 2004, Seol *et al*. 2008, Goodman *et al*. 1972, Kim and Kim 2013). The modeling materials must simultaneously satisfy the required strength and Young's modulus values converted by the reduction rate because they must faithfully represent the physical properties of rocks in the field. However, it is highly difficult to find materials that simultaneously satisfy the required strength and Young's modulus values according to the reduction rate (Kim and Kim 2013). Further, it is difficult to create the desired similar materials by referring to existing studies because the target properties to be reproduced in a scaled model test differ based on the object and purpose of the experiments. Therefore, we need a method to easily reproduce the target properties using materials that are used often.

The mixing ratio of gypsum and sand has a significant effect on the physical properties of the model, which is critical for the success of a simulation test. Hence, the mixing ratio must be determined by testing the target properties at various ratios of gypsum and sand, and many laboratory sample tests should be performed to select a suitable similar material. To this end, this study investigated the physical properties of similar materials by conducting a series of laboratory tests at various mixing ratios of the gypsum, sand, and water as the similar materials of rock. A polynomial model was proposed by configuring a dataset based on the experimental results, and the properties of the gypsum-sand mixture (GSM) were predicted. The proposed polynomial model will help us determine the unconfined compressive strength (UCS), elastic modulus(E), and density, which are important properties of rock modeling materials. Further, the sensitivity of the model to the application range and major influencing factors are evaluated through a statistical analysis of the proposed model.

2. Materials and methods

2.1 Gypsum

Gypsum is a critical material that determines the physical properties of a mixture. Gypsum plaster is a universal material that is inexpensive and readily available. Commercial gypsum contains chemical-bonded water of 1/2 mol and it is produced through hydration hardening to $CaSO_4 \cdot 2H_2O$ by bonding with water. Gypsum can be mixed with water to form any shape, and its long-term strength is not affected by the completion of the chemical hydration (Coquard and Boisetelle 1994). The initial setting time of gypsum mixed with 60 wt% is approximately 25 min. The hardened gypsum is appropriate for simulating the behaviors of rocks such as limestone, shale, mudstone, and soft rock because it shows consistent UCS and Young's modulus (Hobbs 1968). This study used gypsum ($CaSO_4 \cdot 2H_2O$, purity 99%) from Mungyo Plaster Co., Ltd. (Fig. 1). The chemical compositions of the gypsum used in this study are listed in Table 1.

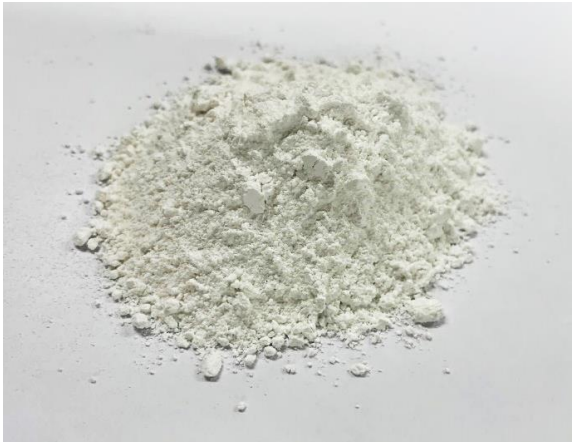

Fig. 1 Physical form of gypsum at the laboratory condition

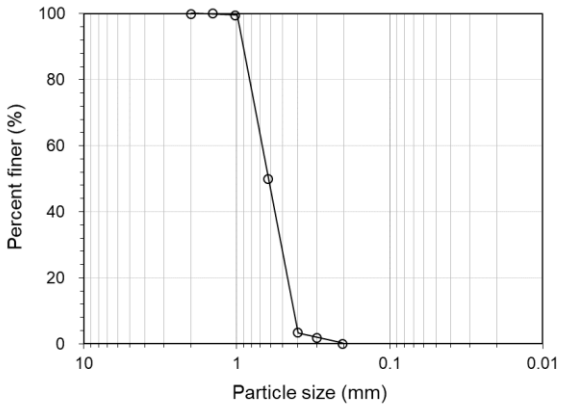

Fig. 2 Particle size distribution curve of sand used (Jumunjin sand)

Table 1 Chemical composition of gypsum plaster (ASTM C471, 1991)

Ingredient (%)	Gypsum
CaO	38.8
SO_3	54.3
Fe_2O_3	0.01
Water of hydration	6.0
Purity	99.11

2.2 Sand

In this study, Jumunjin sand (KSL 5100) was used, which is the most widely adopted sand in South Korea (Chang *et al*. 2015, Park *et al*. 2008, Min and Huy 2010). Jumunjin sand is based on quartz (SiO_2) and it is appropriate for a mixture of modeling materials because it has a constant particle size distribution curve and it is readily available in South Korea. Jumunjin sand is classified as poorly graded sand (SP, ASTM D 2487, 2017)

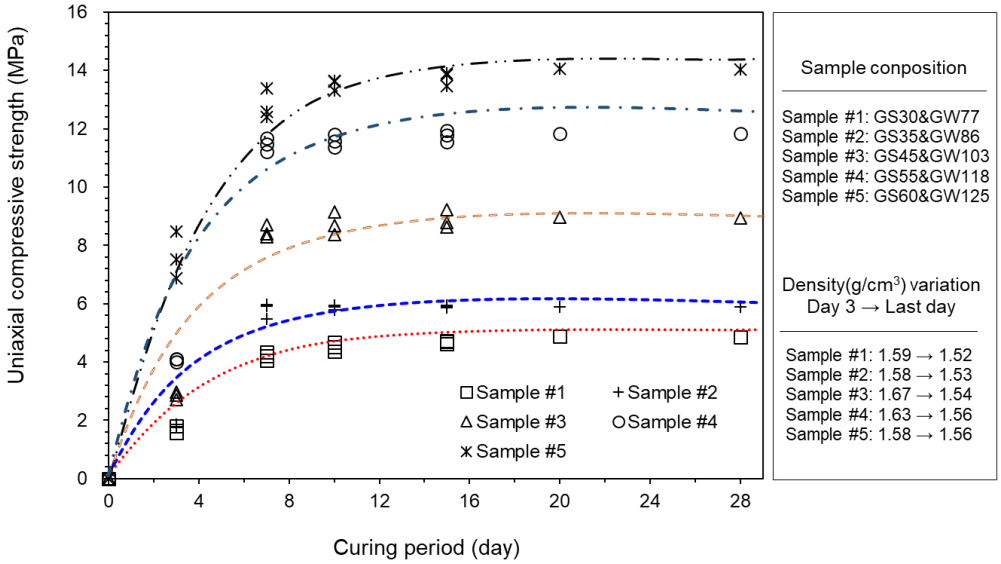

Fig. 3 Variation of UCS with curing period (where GW is the ratio of water to gypsum and GS is the ratio of sand to gypsum. The number after the ratio is the content (%). For example, GS30 means that the percentage of gypsum/sand is 30%)

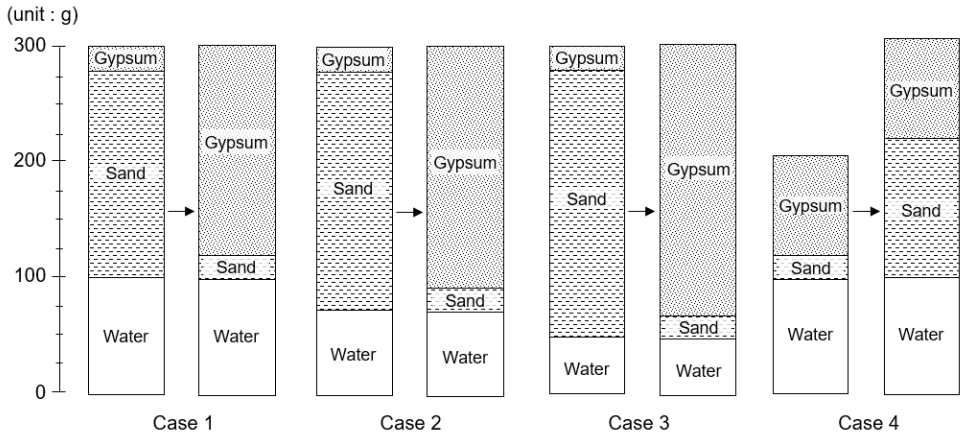

Fig. 4 Case description of laboratory tests

Table 2 Properties of Jumunjin sand

e_{max}	e_{min}	D_{50} (mm)	C_u	C_c	G_s	USCS
0.892	0.644	0.52	1.35	1.14	2.65	SP

with a uniformity coefficient (C_u) and coefficient of gradation (C_c) of 1.35 and 1.14, respectively. Jumunjin sand has a structural composition between e_{min} = 0.64 and e_{max} = 0.89. The particle size distribution curve of Jumunjin sand is shown in Fig. 2.

2.3 Experimental design and test method

This study used a multidisciplinary approach that included laboratory tests, statistical analysis, and computer programming. The UCS was measured after curing for 3, 7, 10, 15, 20, and 28 days at an oven temperature of 50 °C for a wide range of mixing ratios for gypsum, sand, and water to determine the curing time of the sample for laboratory testing. The results confirmed the expression of a constant strength regardless of the mixing ratio after 10 days of curing (Fig. 3). where GW is the ratio of water to gypsum and GS is the ratio of sand to gypsum. The number after the ratio is the content (%). For example, GS30 means that the percentage of gypsum/sand is 30%

Therefore, the basic properties of the model materials used in this study were determined by measuring the UCS and elastic modulus (where elastic modulus refers to the initial tangent modulus) in accordance with the standard test method of ASTM D 2166 (2016) and ASTM D3148-96 (2002) after curing for two weeks at an oven temperature of 50 °C for cylindrical samples with a diameter of 50 mm and a height of 100 mm. Further, the density of the sand in this study indicates the full dry density of GSM. Before loading, the sample was weighed with an accuracy of 0.01 g and the diameter and height were measured with an accuracy of 1

mm. The data of all experiments were taken as the average value of three replicates.

For the mixing methods for gypsum, sand, and water, the component materials for the GSM, four cases are set, as shown in Fig. 4. The total weight is set to 300 g in accordance with the mold volume used. For cases 1, 2, and 3, the ratio of gypsum and sand was changed at fixed intervals, whereas the water weight was fixed at 100 g, 75 g, and 50 g. For Case 4, only the mixed amount of sand was changed, while the weights of the gypsum and water were fixed at 100 g. Therefore, Cases 1, 2, and 3 were designed to examine the changes in the properties of the mixture according to the mixing ratio of gypsum and water and the mixing ratio of gypsum and sand. In other words, gypsum is a gypsum hydrate, and the amount of water it needs to develop strength is chemically determined. Therefore, we want to see how the water reacts with the gypsum and, if excess is added, how it reacts with the sand and affects the overall GSM. Case 4 was designed to examine the changes in the properties of the mixture according to the sand content in a condition of water content with which gypsum can sufficiently react. For the dataset used in this study, the values of UCS, elastic modulus, and density according to the mixing ratio of gypsum, sand, and water were determined by experimenting with 459 cylindrical samples in total using the above method. Further, a polynomial model that can predict the values of physical properties according to the ratio of the mixing materials was proposed using a polynomial approach, and the accuracy of the model was tested using statistical parameters.

2.4 Modeling using polynomial approach

The polynomial model has been applied to many geotechnical problems over the past few years and has achieved successful results to some extent. In the geotechnical field, the polynomial model has been applied to predict the undrain shear strength of clays, pile bearing capacity, liquefaction-induced lateral displacement, shear wave velocity, shear wave velocity, and recompression index of consolidation based on the soil characteristics (Kalantary *et al*. 2009, Ardalan *et al*. 2009, Mola-Abasi *et al*. 2015, Kordnaeij *et al*. 2015). Therefore, this approach can be applied to the empirical correlation of UCS, *E*, and density of the GSM.

The basic assumption is that a pair of input parameters can be connected through a polynomial function to the outputs. Such a representation can be used for input–output mapping. The formal explanation of the identification problem is to find a function F that can be approximately used instead of the observed one f to predict output Y for a given input vector X = (x_1, x_2, x_3, …, x_n) as close as possible to its observed output y. Therefore, for M observations of input data, the single output data pairs are

$$y_i = f\left(x_{i1}, x_{i2}, x_{i3}, \cdots, x_{in}\right) \qquad \left(i = 1, 2, 3, \cdots, M\right) \quad (1)$$

It is possible to use a polynomial model to predict the output values y_i for any given input vector X (x_{i1}, x_{i2}, x_{i3},…, x_{in}), that is

$$Y_i = F\left(x_{i1}, x_{i2}, x_{i3}, \cdots, x_{in}\right) \qquad \left(i = 1, 2, 3, \cdots, M\right) \quad (2)$$

The problem is now to determine a polynomial model such that the square of the differences between the observed and predicted outputs is minimized. Hence

$$Sum\left[F\left(x_{i1}, x_{i2}, x_{i3}, \cdots, x_{in}\right) - y_i\right]^2 \rightarrow \min \quad (3)$$

The general connection between input and output variables can be expressed by a complicated discrete form of the Volterra functional series known as the Kolmogorov–Gabor polynomial (Jamali *et al*. 2008). This full-form mathematical description can be represented by a system of partial quadratic polynomials comprising only two variables in the arrangement of

$$Y = F\left(x_i, y_i\right) = a_0 + a_1 x_i + a_2 y_i + a_3 x_i^2 + a_4 y_i^2 + a_5 x_i y_i \quad (4)$$

Thus, the partial quadratic description is recursively used to build a general mathematical relationship between the inputs and outputs. The coefficients a_i in Eq. (4) are calculated using regression techniques such that the input data are correctly related to the physical properties of the GSM.

3. Test results

3.1 Test results of UCS and E with density

Fig. 5 shows the UCS and *E* for the density of each sample as a result of the experiment in Cases 1, 2, and 3. The UCS and *E* showed similar patterns according to the mixing ratio of gypsum, sand, and water set in each case. A UCS in the range of approximately 0–45 MPa and an *E* in the range of approximately 0–18 GPa can be reproduced with the dihydrate gypsum and sand of the particle size distribution similar to the Jumunjin sand used in this study. Furthermore, materials with various densities can be produced for the same UCS and *E*. Fig. 6(a) shows the relationship between UCS and *E* in Cases 1, 2, and 3. In Fig. 6(b) the *E* value of the GSM increases with the UCS, and they show a linear relationship similar to the relationship between the UCS and *E* of the rock mass (Kumar *et al*. 2017, Sachpazis 1990, Horsrud 2001). Therefore, the GSM in this paper can be considered to have similar physical properties to real rock mass.

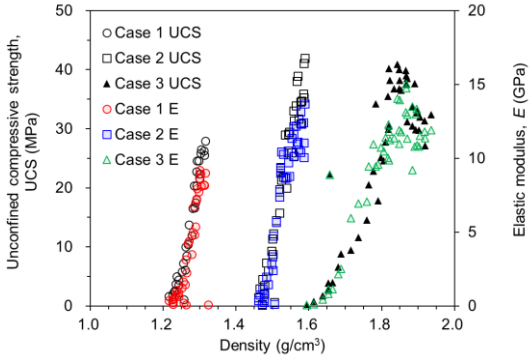

Fig. 5 Effect of uniaxial compressive strength and elastic modulus with density of GSM

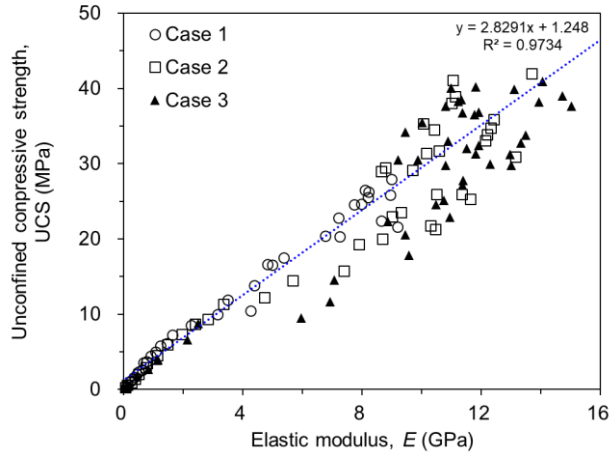

(a) Experimental data from this study

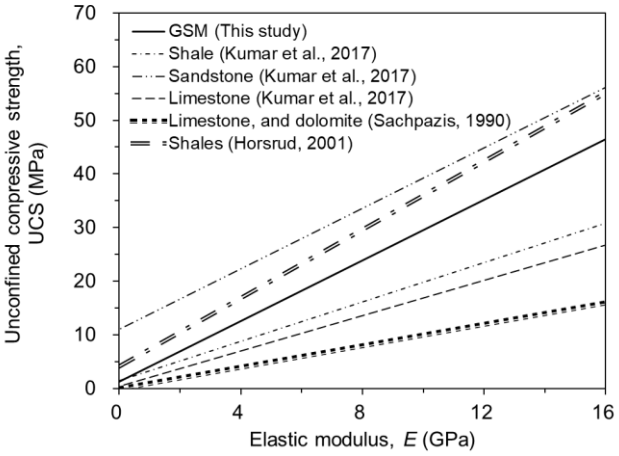

(b) Comparisons with previous studies

Fig. 6 Relationship between uniaxial compressive strength and elastic modulus

3.2 Effect of mixing ratio on UCS

The physical properties of the GSM vary with the mixing ratio of gypsum, sand, and water. Fig. 7 shows the change in the UCS according to the weight ratio of the mixing materials of the GSM. Here, regarding the ratio of the mixing materials, GW denotes the weight ratio of gypsum to water (G/W), GS the weight ratio of gypsum to sand (G/S), and SG the weight ratio of sand to gypsum (S/G). The UCS shows a slightly decreasing trend when the GW ratio exceeds approximately 300 (Fig. 7(a)). Although, the amount of injected water varies by case, and the UCS result is similar if the GW ratio is the same. The UCS may decrease if the weight of gypsum is significantly larger than that of water. Thus, if the amount of water reacting with the gypsum is insufficient, the strength of the gypsum mixture may not be fully developed. The UCS result according to the GS ratio shows that the GS ratio at which the UCS is expressed varies by case (Fig. 7(b)). Overall, the UCS tended to increase with the GS ratio.

In Cases 1, 2, and 3, the UCS shows irregularly changing patterns after the GS ratios of approximately 500, 400, and 150, respectively. Similar to Fig. 7(a), when the GS ratio increases (the amount of gypsum increases), an insufficient amount of water reacting with gypsum can affect the UCS value because of the nonuniform mixing. If the amount of gypsum increases when the amount of water is small, as in Case 3, the UCS may decrease. The density changes according to the SG ratio showed the same pattern in every case; the higher the SG ratio, the smaller is the UCS (Fig. 7(c)). The amount of sand and UCS were negatively correlated. Case 3 exhibited a high SG ratio owing to the small ratio of water. The reason that the UCS appeared differently even at the same SG ratio is that the amount of injected water varies by case. Therefore, the decrease in UCS with increasing SG ratio is because of the relative decrease in the amount of gypsum. In summary, gypsum and water have an important role in the variation of UCS. An increase in sand content relative to gypsum was found to have a decreasing effect on UCS. Therefore, it would be reasonable to set GW and SG ratio as predictors of UCS in GSM.

3.3 Effect of mixing ratio on E

Fig. 8 shows changes in E according to the weight ratio of the mixing materials of the GSM. The change pattern of the properties according to the mixing ratio of materials is

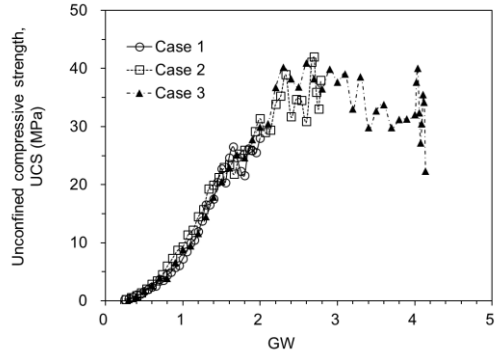

(a)

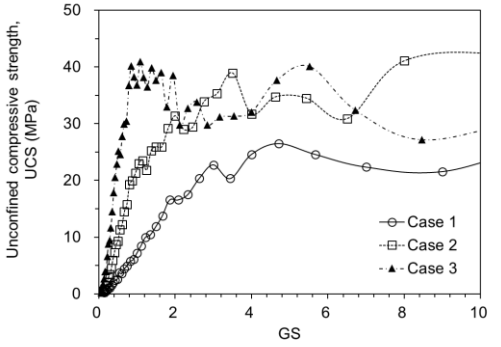

(b)

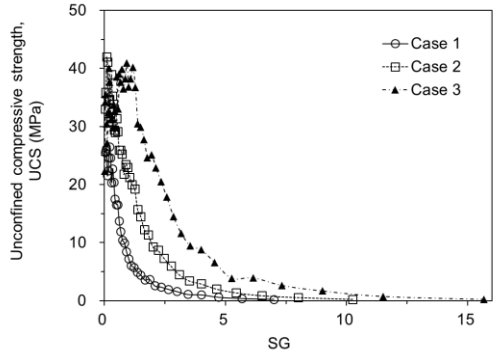

(c)

Fig. 7 Effect of mixing ratio of gypsum, sand and water on unconfined compressive strength (UCS) and: (a) the weight ratio of gypsum to water (GW), (b) the weight ratio of gypsum to sand (GS), and (c) the weight ratio of sand to gypsum (SG)

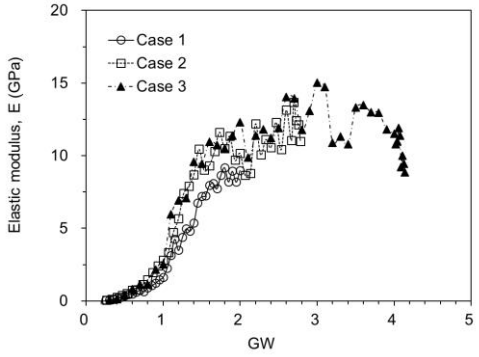

(a)

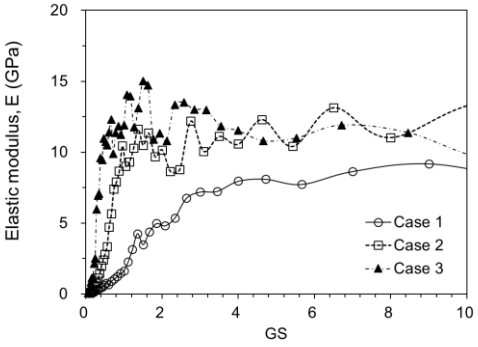

(b)

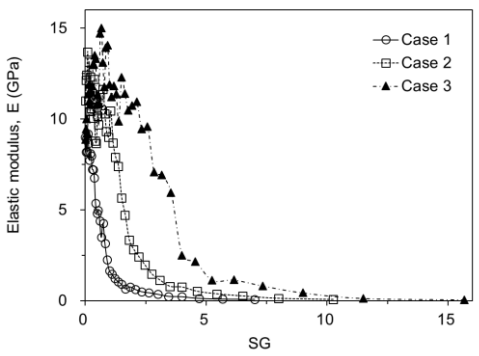

(c)

Fig. 8 Effect of mixing ratio of gypsum, sand and water on elastic modulus (E) and: (a) the weight ratio of gypsum to water (GW), (b) the weight ratio of gypsum to sand (GS), and (c) the weight ratio of sand to gypsum (SG)

the same as the pattern of UCS because the UCS and E have a linear relationship, as shown in Fig. 6. Further, E shows a decreasing trend when the GW ratio becomes larger than approximately 300, and it is influenced by the GW, as in the UCS (Fig. 8(a)). If the materials are mixed at the same GW ratio, the E value becomes similar in every case. Further, E increased with the GS ratio, and after reaching the peak, and it showed an irregular change pattern (Fig. 8(b)). Likewise, because of the different mixing amounts of water by case, it appears to have an adverse effect on the properties if the amount of water is unnecessarily large for a reaction with gypsum. The E value showed a negative correlation with the SG ratio (Fig. 8(c)). The higher the SG ratio, the smaller is the value of E because the amount of gypsum decreases relatively. In the final analysis, similar to UCS, the amount of sand did not significantly affect the expression of E. In the case of E of GSM, GW and SG ratio were set as predictors to express both the increase and decrease of physical properties.

3.4 Effect of mixing ratio on density

The change in the density of the GSM according to the mixing ratio shows a different pattern from that of the UCS and E. Fig. 9 shows the change in the density of the GSM according to the mixing ratio. The density shows an

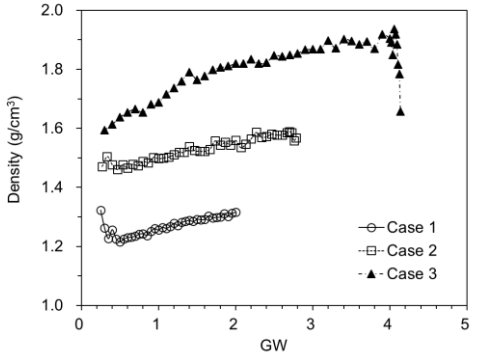

(a)

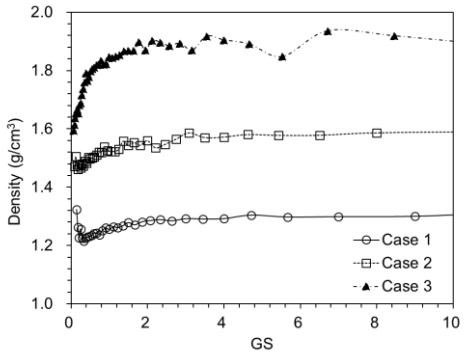

(b)

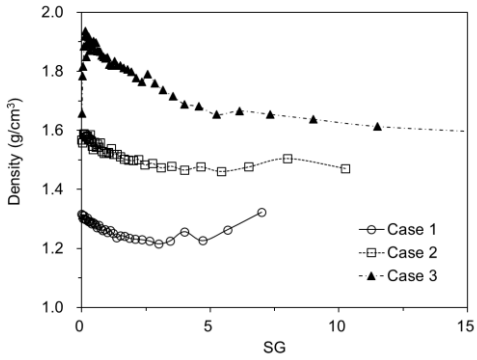

(c)

Fig. 9 Effect of mixing ratio of gypsum, sand and water on density and: (a) the weight ratio of gypsum to water (GW), (b) the weight ratio of gypsum to sand (GS), and (c) the weight ratio of sand to gypsum (SG)

increasing trend according to the GW ratio (Fig. 9(a)), and the increasing amount according to the GW ratio is similar in Cases 1–3. In Case 3, the density shows a change up to a high GW ratio because of the large amount of water; however, the density decreases when the GW ratio becomes larger than approximately 350 because of the insufficient amount of water. The density increases with the GS ratio and gradually stabilizes (Fig. 9(b)). In Cases 1–3, the density increased until the GS ratio became approximately 200 and changed slightly after that. At a GS ratio below 200, the increase in density is different in each case. This suggests that when the gypsum sufficiently reacts with water, the added gypsum does not influence the density.

In contrast, the larger the SG ratio, the smaller is the density (Fig. 9(c)). The effect of density can be observed

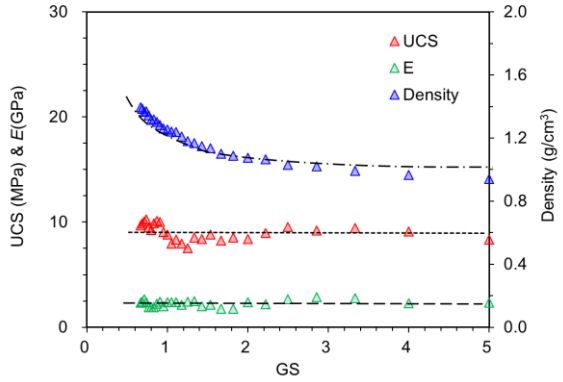

(a)

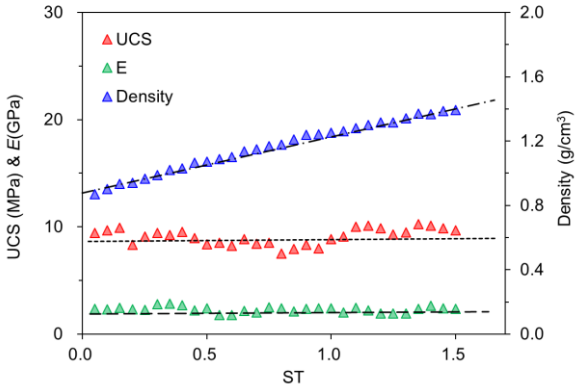

(b)

Fig. 10 Effect of sand content on physical properties with (a) GS ratio and (b) ST ratio

clearly in the results of Case 4. Fig. 10 shows the result of Case 4, where only the mixing amount of sand is different for the same mixing amounts of gypsum and water. Even if the GS ratio increased, the UCS and E were almost constant without significant changes; however, the density showed a decreasing trend (Fig. 10(a)). The decrease in density is a result of the increasing amount of sand. Fig. 10(b) shows the weight ratio of the sand to the total input amount (ST ratio). Because the amounts of gypsum and water are constant, it was represented by the ST ratio to highlight the effect on sand. Thus, the UCS and E remained constant without significant changes as the sand content increased; however, the density increased steadily This suggests that the effect of the GW ratio on the density of the GSM is dominant within the range where the sand content and the characteristics of the UCS and *E* are expressed. Hence, the GW and SG ratios were set as the variables to consider positive and negative effects for predicting the density of GSM.

4. Prediction model and statistical analysis

4.1 Prediction model using polynomial approach

In this study, a polynomial model was configured using a dataset with 459 data points with the mixing ratios of materials that comprise the gypsum–sand mixture as the

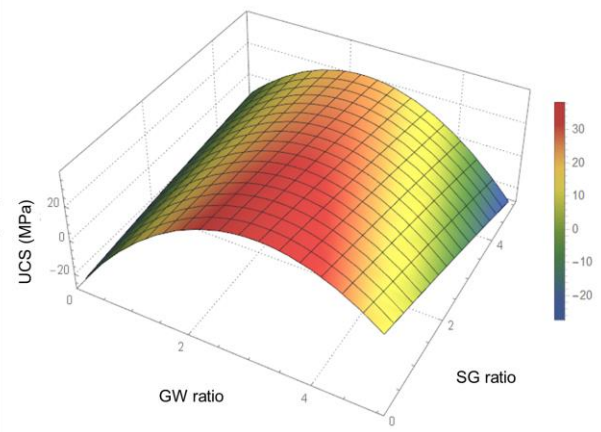

(a)

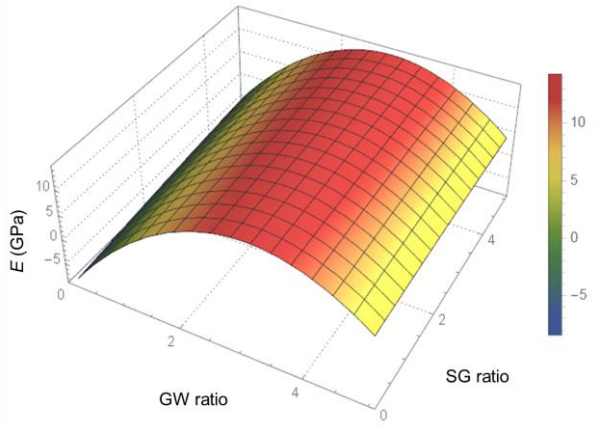

(b)

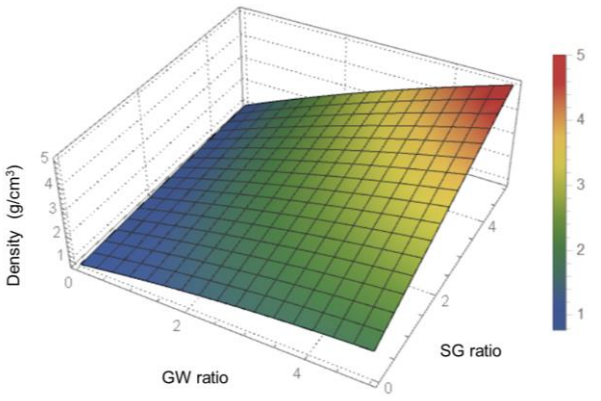

(c)

Fig. 11 Response surface plot of physical properties for GSM: (a) UCS, (b) E and (c) Density

input; the measurements of UCS, E, and density were used as the output. To generate a predictive model using the polynomial approach, we utilized only 75% of the total experimental data, while the remaining 25% was used to validate the proposed model. In this case, the data was equally extracted for each case to prepare a dataset for validation. In this data set, the weight ratios of gypsum, sand, and water expressed as the GW and SG ratios were used as parameters. The correlation between the mixing ratio of the materials and the properties of the GSM can be expressed appropriately by a polynomial model (Volterra series). The corresponding polynomial representations for predicting the UCS, E, and density of the GSM are respectively expressed as

$$UCS = -28.1 + 42.646GW - 6.821GW^2 + 3.876SG - 2.31GW \cdot SG - 0.1468SG^2 \quad (5)$$

$$E = 0.772 + 0.357GW - 0.027GW^2 + 0.0513SG + 0.12GW \cdot SG - 0.00284SG^2 \quad (6)$$

$$Density = 0.772 + 0.3576\mathrm{GW} - 0.027GW^2 + 0.051SG + 0.12GW \cdot SG - 0.0028SG^2 \quad (7)$$

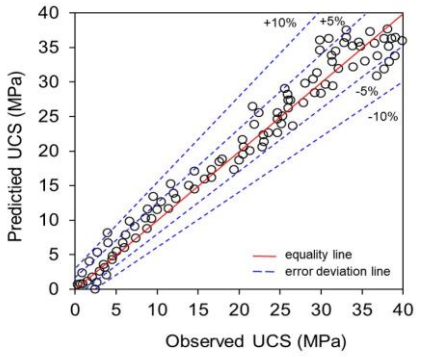

(a)

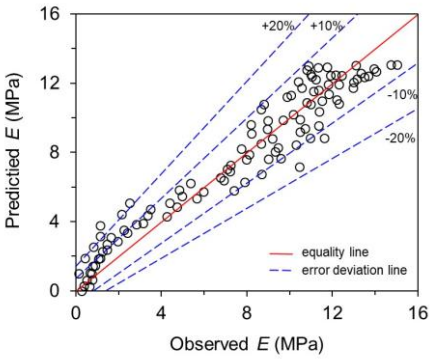

(b)

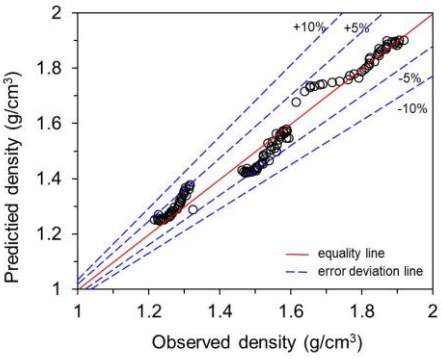

(c)

Fig. 12 Polynomial model predicted physical properties against observed data: (a) UCS, (b) E and (c) density

where GW and SG are the ratios of gypsum to water, sand to gypsum, and gypsum to sand, respectively. From Eqs. (5)-(7), we can estimate the properties of GSM (UCS, *E*, and Density) as two variables, GW and SG. Fig. 11 shows the response surface plot for each property of GSM. It can be seen that UCS and *E* show similar trends, and as GW increases, the physical properties also increase and decrease at some level, which also depends on the change in SG. For density, the magnitude of the increase is more affected by SG than GW. Fig. 12 shows the relationship between the predicted values obtained using the polynomial model and the observed values for validation data sets. The models for predicting the UCS, *E*, and density showed good correlations close to the equality line and appeared to successfully predict the observed values. According to the reliability-based concept of statistical analysis, the predicted and observed values must match completely; however, the accuracy and performance of the model must be evaluated using statistical indices.

4.2 Evaluation of the performance of the model

The performance of polynomial model was estimated by the following measures.

Root mean square error (RMSE)

$$RMSE = \sqrt{\frac{1}{M}\sum_{i=1}^{M}\left(h_i - \bar{h}\right)^2} \tag{8}$$

Coefficient of determination (R^2)

$$R^2 = \left[\frac{\sum_{i=1}^{M}\left(h_i - \bar{h}\right)\left(t_i - \bar{t}\right)}{\sqrt{\sum_{i=1}^{M}\left(h_i - \bar{h}\right)^2 \sum_{i=1}^{M}\left(t_i - \bar{t}\right)^2}}\right]^2 \tag{9}$$

Mean absolute deviation (MAD)

$$MAD = \frac{\sum_{i=1}^{M}\left|h_i - t_i\right|}{M} \tag{10}$$

Mean absolute percentage error (MAPE)

$$MAPE = \frac{\sum_{i=1}^{M}\left|h_i - t_i\right|}{\sum_{i=1}^{M} h_i} \times 100 \tag{11}$$

where M, h_i, $\bar{h}$, t_i, and t denote the number of observations, ith observed value, mean h value, ith predicted value, and mean t value, respectively. Table 3 summarizes the predicted performance of the polynomial model using the above statistical indices. Lower values for RMSE, MAD, and MAPE provided better performance. In fact, for a precise error-free model, one can expect R^2 equal to one, RMSE, MAD, and MAPE equal to zero. In other words, the lower the RMSE, MAPE, and MAD, the higher is the performance of the model.

The result of modeling UCS, *E*, and density using the polynomial model and coefficients of determination (R^2) were 0.987, 0.979, and 0.999, respectively. The parameters of the model showed good correlations with the target properties. The MAPE, RMSE, and MAD of the prediction model for the properties of the GSM were mostly low, which indicates a satisfactory performance.

Table 3 Statistical results for the polynomial model of physical properties

Model for physical properties	MAPE	RMSE	MAD	R^2
UCS	10.61	2.73	2.10	0.987
E	14.44	1.22	1,00	0.979
Density	2.03	0.04	0.03	0.999

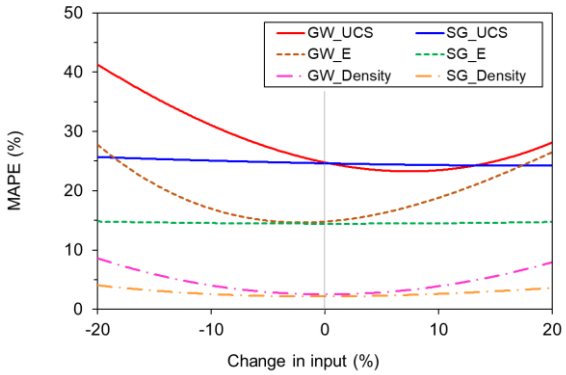

Fig. 13 Effect of measured error of input parameters on the MAPE of the predicted physical properties

4.3 Sensitivity analysis

In this study, various input parameters were changed at a constant rate for the prediction model for the properties of the GSM; their effects on the error of the output values were examined. To that end, the MAPE data of the observed and predicted values were calculated using Eq. (11) while changing each parameter of the sample in the range of ±20% and maintaining other parameters constant; the results are shown in Fig. 13. The UCS and *E* of GSM show high MAPEs according to the change in the GW ratio, and these errors significantly affect the results. For example, if the GW ratio is measured and used inaccurately with a -10% error, an error of approximately 30% can occur in the prediction of UCS. One notable thing is that the results are affected differently depending on whether the input changes in a positive or negative direction. In the case of UCS, the impact is greater when the GW ratio changes in the negative direction. However, a positive change will have a relatively small impact. The MAPE changed very little when the SG ratio was changed, which indicates an insignificant effect on the UCS and *E* values of the GSM. The resulting density of the GSM was affected by the change in the input parameters. For instance, if the GW ratio has a 10% error, the predicted density can have a mean error of 4.35%.

A sensitivity analysis was used to identify the significance of each input parameter on the objective (output) parameter in the model. The cosine amplitude method (CAM) is a sensitivity analysis method used to

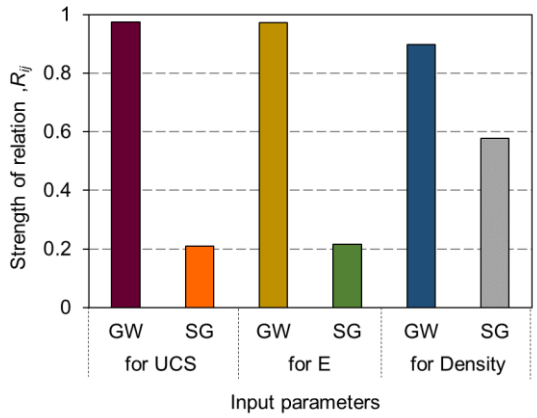

Fig. 14 Strength of relation (R_{ij}) between physical property and input parameters

obtain express similarity relations between the related parameters (Yang and Zhang 1997, Vu-Bac *et al.* 2014). All data pairs were expressed in the common X-space to apply this method. The data pairs used to construct a data array X are defined as

$$X = \{x_1, x_2, x_3, \cdots, x_m\} \tag{12}$$

where x_i denotes a vector with a length of m, which is shown as

$$X_i = \{x_{i1}, x_{i2}, x_{i3}, \cdots, x_{im}\} \tag{13}$$

Thus, each of the data pairs can be thought of as a point in the m-dimensional space, where each point requires m coordinates for a full description. Each element of a relation, R_{ij}, results in a pairwise comparison of two data pairs. Therefore, the strength of the relation between the data pairs x_i and x_j is given by

$$R_{ij} = \frac{\sum_{k=1}^{m} x_{ik} x_{jk}}{\sqrt{\sum_{k=1}^{m} x_{ik}^2 \sum_{k=1}^{m} x_{jk}^2}} \tag{14}$$

The strengths of the relations (R_{ij} values) between the physical property (output) and input parameters using the CAM method are shown in Fig. 14. Fig. 14 shows the strength of the relation of each parameter for the properties of the GSM. This sensitivity analysis was conducted based on the experimental dataset used in this study. The GW ratio has the largest effect on the UCS, E, and density of GSM in the evaluated data range. The SG ratio is highly correlated with density, and relatively low for UCS and E. Similar to the previous experimental results, for UCS and E, the GW ratio is more highly correlated than the SG ratio, and density is highly correlated with both GW and SG.

5. Conclusions

In this study, the UCS, E, and density of 459 GSM samples were measured through laboratory tests, and based on these data, a polynomial model was developed with the mixing ratio of gypsum, sand, and water as the parameter to enable the prediction of the properties of the GSM. The findings of this study can be summarized as follows.

- The target properties of the GSM desired by the user can be reproduced by adjusting the weight ratio of the mixing materials, that is, gypsum, sand, and water, which can be used as modeling materials for simulating rocks or complex substance.
- The parameter that has the largest effect on the properties of GSM is the GW ratio (ratio of gypsum to water), and a sufficient amount of gypsum is required for the reaction with water. If the amount of gypsum is greater than the amount required for the reaction, the UCS and E values tended to decrease. Hence, the GW ratio must be adjusted to an appropriate level. The density of GSM is affected by the content of sand, and if the added amount of gypsum is larger than the amount required for the reaction, the density of GSM is affected to some degree. On the other hand, higher sand content has a negative impact on UCS and E properties, so this should also be considered. Therefore, the UCS and E of the GSM can be predicted using the GW and SG ratios as parameters; the density using GW and SG ratios as the parameters.
- The error bias of the polynomial model that can predict the properties of GSM was less than 3%, and the R^2 values between the observed and predicted values of the prediction model for the UCS, E, and density of GSM based on the experimental data for validation were 0.987, 0.979, and 0.999, respectively. These results suggest excellent correlations between the model parameters and target properties.
- The results of the sensitivity analysis that examined the effects of output on the input of the prediction model for the properties of GSM showed that the UCS and E of the GSM were significantly affected by the GW ratio, whereas the effect of change in input values on the density was insignificant.
- The results of the analysis of the parameters using the CAM method showed that the factor that had the largest effect on the properties of the GSM was the GW ratio, whereas the SG ratio had a relatively low effect.
- The polynomial model in this study has an excellent ability to predict the UCS, E, and density of the GSM more simply and economically than expensive laboratory procedures. Therefore, it will provide great assistance in inversely determining the weight ratio of mixing materials for the target properties and using them as modeling materials.

Acknowledgments

This research was supported by a grant from the project "Development of Smart Complex Solution for Large-Deep Underground Space Using Artificial Intelligence (20230105-001)", which was funded by the Korea Institute of Civil Engineering and Building Technology.

References

Ardalan, H., Eslami, A. and Nariman-Zadeh, N. (2009), "Piles shaft capacity from CPT and CPTu data by polynomial neural networks and genetic algorithms", *Comput. Geotech*., **36**(4), 616-625. https://doi.org/10.1016/j.compgeo.2008.09.003.

ASTM C471 (1991), Standard Test Methods for Chemical Analysis of Gypsum and Gypsum Products, ASTM International; West Conshohocken, PA, USA.

ASTM D2166 / D2166M-16 (2016). Standard Test Method for Unconfined Compressive Strength of Cohesive Soil, ASTM International; West Conshohocken, PA, USA.

ASTM D2487 (2017), Standard Practice for Classification of Soils for Engineering Purposes (Unified Soil Classification System), ASTM International; West Conshohocken, PA, USA.

ASTM D3148-96 (2002), Standard Test Method for Elastic Moduli of Intact Rock Core Specimens in Uniaxial Compression, ASTM International; West Conshohocken, PA, USA.

Chapman, D.N., Ahn, S.K., Hunt, D.V.L. and Chan, A.H.C. (2006), "The use of model tests to investigate the ground displacements associated with multiple tunnel construction in soil", *Tunn. Undergr. Sp. Tech.*, **21**(3), 413. https://doi.org/10.1016/j.tust.2005.12.059.

Chen, S., Wang, H., Zhang, J., Xing, H. and Wang, H. (2015), "Experimental study on low-strength similar-material proportioning and properties for coal mining", *Adv. Mater. Sci. Eng*., **24**(5), 457-470. https://doi.org/10.1155/2015/696501.

Chung, J., Moon, I. and Yoo, C. (2013), "Behaviour characteristics of tunnel in the cavity ground by using scale model tests", *J. Kor. Geoenviron. Soc*., **14**(12), 61-69. http://dx.doi.org/10.14481/jkges.2013.14.12.061.

Coquard, P. and Boistelle, R. (1994), "Water and solvent effects on the strength of set plaster", *Int. J. Rock Mech. Min. Sci. Geomech. Abstr*., **31**(5), 517-524. https://doi.org/10.1016/0148-9062(94)90153-8.

Conley, R.F. and Bundy, W.M. (1958), "Mechanism of gypsification", *Geochimica et Cosmochimica Acta*., **15**(1-2), 57-72. https://doi.org/10.1016/0016-7037(58)90010-3.

Chang, I., Prasidhi, A.K., Im, J. and Cho, G.C. (2015), "Soil strengthening using thermo-gelation biopolymers", *Constr. Build. Mater*., 77, 430-438. https://doi.org/10.1016/j.conbuildmat.2014.12.116.

Dong, J.Y., Yang, J.H., Yang, G.X., Wu, F.Q. and Liu, H.S. (2012), "Research on similar material proportioning test of model test based on orthogonal design", *J. China Coal Soc*., **37**(1), 44-49.

Goodman, R.E., Heuz, F.E. and Bureau, G.J. (1972), "On modelling techniques for the study of tunnels in jointed rock", *Proceedings of the 14th US Symp. Rock Mech.* OnePetro. University Park, U.S.A., June. https://doi.org/10.1016/0148-9062(74)90327-1.

Harris, H.G. and Sabnis, G. (1999), *Structural Modeling and Experimental Techniques*, 2nd Ed., CRC press.

He, M.C., Gong, W.L., Zhai, H.M. and Zhang, H.P. (2010), "Physical modeling of deep ground excavation in geologically horizontal strata based on infrared thermography", *Tunn. Undergr. Sp. Tech.*. **25**(4), 366-376. https://doi.org/10.1016/j.tust.2010.01.012.

Hobbs, D.W. (1968), "Scale model study of strata movement around mine roadways: I. the dependence of roadway closure upon rock strength", *Int. J. Rock Mech. Min. Sci*., **5**(3), 225-235. https://doi.org/10.1016/0148-9062(68)90010-7.

Horsrud, P. (2001), "Estimating mechanical properties of shale from empirical correlations", *SPE Drill.Complet*., **16**(2), 68-73 https://doi.org/10.2118/56017-PA.

Huang, F., Zhu, H., Xu, Q., Cai, Y. and Zhuang, X. (2013), "The effect of weak interlayer on the failure pattern of rock mass around tunnel–Scaled model tests and numerical analysis", *Tunn. Undergr. Sp. Tech.*, **35**, 207-218. http://dx.doi.org/10.1016/j.tust.2012.06.014.

Indraratna, B. (1990), "Development and applications of a synthetic material to simulate soft sedimentary rocks", *Geotechnique*, **40**(2), 189-200. https://doi.org/10.1680/geot.1990.40.2.189.

Indraratna, B., Haque, A. and Aziz, N. (1998), "Laboratory modelling of shear behaviour of soft joints under constant normal stiffness conditions", *Geotech. Geol. Eng*., **16**(1), 17-44. https://doi.org/10.1023/A:1008880112926

Jamali, A., Nariman-zadeh, N., Darvizeh, A., Ma- soumi, A. and Hamrang, S. (2008), "Multi-objective evolutionary optimization of polynomial neural networks for modelling and prediction of explosive cutting process", *Eng. Appl. Artifi. Int.,* **22**(4-5), 676-687. https://doi.org/10.1016/j.engappai.2008.11.005.

Jeon, S., Kim, J., Seo, Y. and Hong, C. (2004), "Effect of a fault and weak plane on the stability of a tunnel in rock - a scaled model test and numerical analysis", *Int. J. Rock Mech. Min. Sci*., **41**(3), 658-663. https://doi.org/10.1016/j.ijrmms.2004.03.115.

Jiang, Y.J., Xiao, J., Tanabashi, Y. and Mizokami, T. (2004), "Development of an automated servo-controlled direct shear apparatus applying a constant normal stiffness condition", *Int. J. Rock. Mech. Min. Sci*., **41**(2), 275-286. https://doi.org/10.1016%2Fj.ijrmms.2003.08.004.

Johnston, I.W. and Choi, S.K. (1986), "A synthetic soft rock for laboratory model studies", *Geotechnique*, **36**(2), 251-263. https://doi.org/10.1680/geot.1986.36.2.251.

Jung, H.R. and Kim, J.W. (2006), "Deformation behaviors around tunnel in anisotropic rocks considering joint orientation and rock pressure condition using scaled model tests", *Tunn. Undergr. Sp*., **16**(4), 313-325.

Karni, J. (1970), "Sand for gypsum-sand plaster", *Matériaux et Construction*, **3**(4), 261-268. https://doi.org/10.1007/BF02474014.

Kalantary, F., Ardalan, H. and Nariman-Zadeh, N. (2009), "An investigation on the Su–NSPT correlation using GMDH type neural networks and genetic algorithms", *Eng. Geol*., **104**(1-2), 144-155. https://doi.org/10.1016/j.enggeo.2008.09.006.

Kim, P.G. and Kim, J.W. (2013), "Scale model studies for stability estimation of twin tunnels with small clearance", *Tunn. Undergr. Sp*., **23**(2), 130-140. https://doi.org/10.7474/TUS.2013.23.2.130.

Kim, S.H., Burd, H.J. and Milligan, G.W.E. (1998), "Model testing of closely spaced tunnels in clay", *Geotechnique*, **48**(3), 375-388. https://doi.org/10.1680/geot.1998.48.3.375.

Kordnaeij, A., Kalantary, F., Kordtabar, B. and Mola-Abasi, H. (2015), "Prediction of recompression index using GMDH-type neural network based on geotechnical soil properties", *Soils Found*., **55**(6), 1335-1345. https://doi.org/10.1016/j.sandf.2015.10.001.

Kumar R., Bhargava, K. and Choudhury, D. (2017), "Correlations of uniaxial compressive strength of rock mass with conventional strength properties through random number generation", *Int. J. Geomech.*, **17**(2), 06016021. https://doi.org/10.1061/(ASCE)GM.1943-5622.0000716

Lemaitre, J. (1985), "A continuous damage mechanics model for ductile fracture", *J. Eng. Mater. Technol*., **107**(1), 83-89. https://doi.org/10.1115/1.3225775.

Lee, J. and Jeong, S. (2016), "Experimental study of estimating the subgrade reaction modulus on jointed rock foundations", *Rock Mech. Rock Eng*., **49**(6), 2055-2064. https://doi.org 10.1007/s00603-015-0905-9.

Liu, J., Feng, X.T., Ding, X.L., Zhang, J. and Yue, D.M. (2003), "Stability assessment of the three-gorges dam foundation,

China, using physical and numerical modeling, part I: Physical model tests", *Int. J. Rock Mech. Min. Sci.*, **40**(5), 609-631. https://doi.org/10.1016/S1365-1609(03)00055-8.

Ma, F.P., Li, Z.K. and Luo, G.F. (2004), "NIOS model material and its use in geo-mechanical similarity model test", *J. Hydroelectr. Eng*., **23**(1), 48-51.

Manzella, I. and Labiouse, V. (2008), "Qualitative analysis of rock avalanches propagation by means of physical modeling of non-constrained gravel flows", *Rock Mech. Rock Eng.*, **41**(1), 133-151. https://doi.org/10.1007/s00603-007-0134-y.

Min, T.K. and Huy, P.T. (2010), "A soil-water hysteresis model for unsaturated sands based on fuzzy set plasticity theory", *KSCE J. Civil Eng*., **14**(2), 165-172. https://doi.org/10.1007/s12205-010-0165-x.

Mola-Abasi, H., Dikmen, U. and Shooshpasha, I. (2015), "Prediction of shear-wave velocity from CPT data at Eskisehir (Turkey), using a polynomial model", *Near Surface Geophy*., **13**(2), 155-168. https://doi.org/10.3997/1873-0604.2015010.

Park, L.K., Suneel, M. and Chul, I.J. (2008), "Shear strength of Jumunjin sand according to relative density", *Mar. Georesour. Geotec*., **26**(2), 101-110. https://doi.org/10.1080/10641190802022445.

Sachpazis, C.I. (1990), "Correlating Schmidt hardness with compressive strength and Young's modulus carbonate rocks", *Bull. Int. Assoc. Eng. Geol.*, **42**(1), 75-83. https://doi.org/10.1007/BF02592622

Seo, S., Lim, H. and Chung, M. (2021), "Evaluation of failure mode of tunnel-type anchorage for a suspension bridge via scaled model tests and image processing", *Geomech. Eng*., **24**(5), 457-470. https://doi.org/10.12989/gae.2021.24.5.457.

Seol, H., Jeong, S., Cho, C. and You, K. (2008), "Shear load transfer for rock-socketed drilled shafts based on borehole roughness and geological strength index (GSI)", *Int. J. Rock Mech. Min. Sci*., **45**(6), 848-861. https://doi.org/10.1016/j.ijrmms.2007.09.008.

Sterpi, D. and Cividini, A. (2004), "A physical and numerical investigation on the stability of shallow tunnels in strain softening media", *Rock Mech. Rock Eng*., **37**(4), 277-298. https://doi.org/10.1007/s00603-003-0021-0.

Stimpson, B. (1970), "Modelling materials for engineering rock mechanics", *Int. J. Rock Mech. Min. Sci. Geomech. Abstr*., **7**(1), 77-121. https://doi.org/10.1016/0148-9062(70)90029-X.

Vu-Bac, N., Lahmer, T., Zhang, Y., Zhuang, X. and Rabczuk T. (2014), "Stochastic predictions of interfacial characteristic of polymeric nanocomposites (PNCs)", *Compos. Part B, Col. Eng*., **59**, 80-95. https://doi.org/10.1016/j.compositesb.2013.11.014.

Yang Y. and Zhang Q. (1997), "A hierarchical analysis for rock engineering using artificial neural networks", *Rock Mech. Rock Eng*., **30**(4), 207-222. https://doi.org/10.1007/BF01045717.

Yang, Z.Y. and Chiang, D.Y. (2000), "An experimental study on the progressive shear behavior of rock joints with tooth-shaped asperities", *Int. J. Rock Mech. Min. Sci.*, **37**(8), 1247-1259. http://dx.doi.org/10.1016/S1365-1609(00)00055-1.

Zhang, Q.Y., Li, S.C., Guo, X.H., Li, Y. and Wang, H.P. (2008), "Research and development of new typed cementitious geotechnical similar material for iron crystal sand and its application", *Rock Soil Mech.*, **29**(8), 2126-2130.